Numerical study of the phase transitions in the two-dimensional Z(5) vector model

O. Borisenko,[1,*] G. Cortese,[2,†] R. Fiore,[2,‡] M. Gravina,[3,4,§] and A. Papa[2,∥]

[1]*Bogolyubov Institute for Theoretical Physics, National Academy of Sciences of Ukraine, 03680 Kiev, Ukraine*
[2]*Dipartimento di Fisica, Università della Calabria, and Istituto Nazionale di Fisica Nucleare, Gruppo Collegato di Cosenza, I-87036 Arcavacata di Rende, Cosenza, Italy*
[3]*Laboratoire de Physique Théorique d'Orsay, Université de Paris-Sud 11, Bâtiment 210, 91405 Orsay Cedex, France*
[4]*Department of Physics, University of Cyprus, P.O. Box 20357, 1678 Nicosia, Cyprus*

We investigate the critical properties of the two-dimensional Z(5) vector model. For this purpose, we propose a cluster algorithm, valid for Z(N) models with odd values of N. The two-dimensional Z(5) vector model is conjectured to exhibit two phase transitions with a massless intermediate phase. We locate the position of the critical points and study the critical behavior across both phase transitions in details. In particular, we determine various critical indices and compare the results with analytical predictions.

I. INTRODUCTION

The Berezinskii-Kosterlitz-Thouless (BKT) phase transition is known to take place in a variety of two-dimensional (2D) systems: certain spin models, two-dimensional Coulomb gas, sine-Gordon model, solid-on-solid (SOS) model, etc., with the most popular and elaborate case being the two-dimensional XY model [1–3]. There are several indications that this type of phase transition is not a rare phenomenon in gauge models at finite temperature. One can argue that in some three-dimensional lattice gauge models the deconfinement phase transition is of BKT type as well. Here we are going to study an example of a lattice spin model where this type of transition is exhibited, namely, the 2D Z(N) spin model, also known as the vector Potts model.

Consider a 2D lattice $\Lambda = L^2$ with linear extension L and impose periodic boundary conditions on spin fields in both directions. The partition function of the model can be written as

$$Z(\Lambda,\beta) = \left(\prod_{x \in \Lambda} \frac{1}{N} \sum_{s(x)=0}^{N-1} \right) \left\{ \prod_{x \in \Lambda} \prod_{n=1,2} Q[s(x) - s(x+e_n)] \right\}. \tag{1}$$

In the standard formulation the most general Z(N)-invariant Boltzmann weight with $N-1$ different couplings is

$$Q(s) = \exp\left(\sum_{k=1}^{N-1} \beta_k \cos \frac{2\pi k}{N} s \right). \tag{2}$$

In the Villain formulation the Boltzmann weight reads instead

$$Q(s) = \sum_{m=-\infty}^{\infty} \exp\left[-\frac{1}{2}\beta \left(\frac{2\pi}{N} s + 2\pi m \right)^2 \right]. \tag{3}$$

Some details of the critical behavior of 2D Z(N) spin models are well known (see the review in Ref. [4]). The Z(N) spin model in the Villain formulation (3) has been studied analytically in Refs. [5–9]. It was shown that the model has at least two phase transitions when $N \geqslant 5$. The intermediate phase is a massless phase with powerlike decay of the correlation function. The critical index η has been estimated both from the renormalization group (RG) approach of the Kosterlitz-Thouless type and from the weak-coupling series for the susceptibility. It turns out that $\eta(\beta_c^{(1)}) = 1/4$ at the transition point from the strong-coupling (high-temperature) phase to the massless phase (i.e., the behavior is similar to that of the XY model). At the transition point $\beta_c^{(2)}$ from the massless phase to the ordered low-temperature phase one has $\eta(\beta_c^{(2)}) = 4/N^2$. A rigorous proof that the BKT phase transition does take place, and therefore that the massless phase exists, has been constructed in Ref. [10] for both Villain and standard formulations (with one nonvanishing coupling β_1). Monte Carlo simulations of the standard version with $N = 6, 8, 12$ were performed in Ref. [11]. Results for the critical index η agree well with the analytical predictions obtained from the Villain formulation of the model.

In this paper we thoroughly investigate the case $N = 5$, the lowest number where the BKT transition is expected. In particular, we concentrate on the standard formulation [Eq. (2)] with one nonzero coupling β_1. The motivation of our study is threefold: (i) to compute critical indices at the transition points, which could serve as checking points of universality; (ii) to shed light on the discrepancy in the literature concerning the Z(5) model; and (iii) to develop and test a version of the Monte Carlo cluster algorithm that is valid for odd values of N.

The first motivation is related to the study of the finite-temperature transitions in 3D Z(N) and SU(N) lattice gauge theory (LGT). It is expected that in 3D Z(N) LGT a deconfinement phase transition takes place at finite temperature. There is no precise statement about the order of the phase transition, but presumably it is of the BKT type if $N > 4$. If this is the case, the Svetitsky-Yaffe conjecture [12] implies that the 3D Z(N) LGT is in the universality class of the 2D vector Potts model. Moreover, it can be proven that in the strong-coupling

*oleg@bitp.kiev.ua
†cortese@cs.infn.it
‡fiore@cs.infn.it
§gravina@ucy.ac.cy
∥papa@cs.infn.it

region with respect to the spatial coupling, the 3D Z(N) LGT reduces to a 2D Z(N) model with the general Boltzmann weight [Eq. (2)], and such that $\beta_1 = \beta_4 \gg \beta_2 = \beta_3$, for $N = 5$. Here, β_k are effective couplings which depend on the gauge coupling and the temporal extension N_t. Thus, our Z(5) model represents a good approximation to 3D Z(5) LGT in this region.

Next, let $W(x) \in \mathrm{SU}(N)$ and consider the following effective action in 2D

$$S_{\mathrm{eff}} = \sum_{x,n} \mathrm{Tr}W(x)\mathrm{Tr}W^\dagger(x + e_n) + \mathrm{c.c.} \qquad (4)$$

The effective action [Eq. (4)] can be regarded as the simplest effective model for the Polyakov loop which can be derived in the strong-coupling region of 3D SU(N) LGT at finite temperature. It possesses Z(N) global symmetry and thus may well exhibit the BKT transitions which belong to the universality class of the corresponding vector Potts model. Therefore, our investigation here can be viewed as a preliminary step in studying deconfinement phase transition in 3D Z(N) and SU(N) LGTs.

The second motivation reflects the fact that many features of the critical behavior of the Z(5) model are not reliably established. Moreover, there are certain discrepancies even in determining the nature of the phase transition (i.e., whether the phase transition is of BKT type or not).

To summarize the current situation:

(i) The rigorous proof of the massless phase existence in 2D Z(N) models utilizes methods which do not allow the exact value of N to be established, above which the BKT phase transition exists [10].

(ii) Reliable analytical calculations can only be performed with the Villain formulation [Eq. (3)]. The RG study of Ref. [5] predicts that the massless phase exists for all $N > 4$.

(iii) Some information on the phase structure of the general Z(N) spin models can be obtained through the duality transformations (Ref. [13]). These transformations cannot be used to establish the position of the critical points in the Z(5) model [14]. However, duality transformations relate the two critical points and thus can be used to verify the accuracy of numerical data. Moreover, one can predict an approximate phase diagram and argue that the massless phase and the BKT transition exist for $N = 5$ in a certain region of the parameter space [15,16]. The rigorous proof of the existence of the massless phase, constructed in Ref. [15] for the generalized Villain formulation, is particularly important in this context. This generalized formulation contains the vector Potts model defined in Eq. (2) with one nonzero coupling β_1 as a particular case. For completeness we mention that in Ref. [17] it was suggested that there is only one first-order phase transition in the Z(5) model. This, however, contradicts the rigorous results of [15].

(iv) An analytical prediction for the critical index η has been obtained for the Villain formulation in Ref. [5]: $\eta(\beta_c^{(1)}) = 1/4$ and $\eta(\beta_c^{(2)}) = 0.16$ (for $N = 5$). The situation remains unclear for the index ν which governs the behavior of the correlation length. Normally, the value of ν can be estimated from the solution of the RG equations as in the XY model [3]. The analytical solution of the system of RG equations for Z(N) vector models is unknown [5]. Therefore, strictly speaking, there are no strong theoretical arguments indicating

that $\nu = 1/2$, similarly to the XY model. Moreover, the strong-coupling expansion of the Z(5) model combined with Padé approximants predicts that $\nu \approx 0.22$ [5].

(v) Monte Carlo simulations of the Z(N) model have been performed in Refs. [11,18–20]. The results of Ref. [18], though obtained on rather small lattices, indicate that the BKT transition takes place in models with $N \geqslant 8$. This contradicts the results of [11,20] which are in good agreement with the BKT behavior for $N = 6$.

However, most recent simulations of the helicity modulus in the Z(5) model at $\beta_c^{(1)}$ do not agree with what is expected at the BKT transition [19]. Namely, at the critical point the helicity modulus is expected to jump discontinuously to zero, and the jump is observed for the Z(6) model, while in Z(5) the helicity modulus stays small but nonvanishing in the high-temperature region $\beta < \beta_c^{(1)}$.

Still, it remains unclear how this behavior of the helicity modulus influences other features of the BKT transition. The key feature of the massless BKT phase in Z(N) models is the enhancement of the discrete symmetry of the Hamiltonian— the symmetry of the ground state in the intermediate phase is U(1) rather than Z(N) [10]. This can be seen in the characteristic distribution of the complex magnetization, in the powerlike decay of the correlation functions in the massless phase, in the vanishing of the beta function, etc. Also, on the basis of the universality one could conjecture that the critical indices in the Z(5) model are the same both in the standard and Villain formulations. We are not aware of any numerical calculations of these quantities in Z(5). Here, we would like to fill this gap by computing various quantities and extracting critical indices at both transitions. Among the main quantities calculated in this paper are Binder cumulants. As RG invariant quantities, Binder cumulants are very useful in locating the critical couplings and determining the nature of the phase transition. Indeed, the computation of Binder cumulants proved to be very efficient in studying BKT transitions in a variety of models, like the XY model, the discrete Gaussian model, and the SOS model [21]. We therefore believe that these cumulants are also of great value in the investigation of phase transitions in 2D Z(N) models. Preliminary results of our study have been presented in Ref. [22].

This paper is organized as follows: in Sec. II we describe the setup of the Monte Carlo simulation and the cluster

TABLE I. Cluster versus heat-bath in Z(5) on a 64^2 lattice at three values of β: autocorrelation time τ for three observables (energy, magnetization M_L, and population S_L), number of thermalization sweeps, and computer time for 50 000 updates.

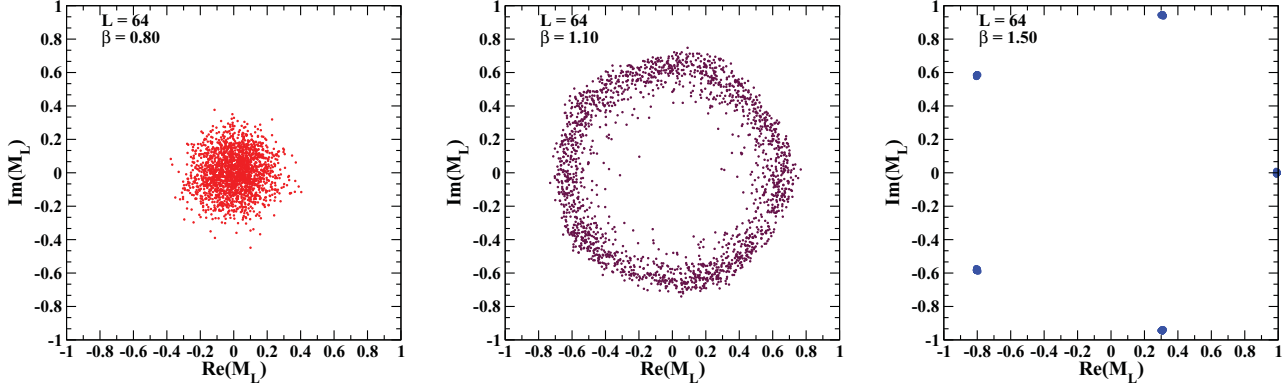|	Energy	M_L	S_L	Thermalization	Time
		$\beta = 0.80$			
cluster	5.135(82)	1.528(38)	1.494(39)	∼10	46.69 s
heat-bath	5.43(33)	12.83(27)	12.65(28)	∼100	1290 s
		$\beta = 1.10$			
cluster	7.36(11)	5.56(10)	7.18(11)	∼10	45.14 s
heat-bath	10.11(48)	48.3(4.8)	60.6(6.1)	∼1000	1194 s
		$\beta = 1.50$			
cluster	8.97(17)	8.71(17)	8.84(17)	∼100	42.60 s
heat-bath	2.38(12)	3.73(15)	3.78(13)	∼6500	1064 s

FIG. 1. (Color online) Scatter plot of the complex magnetization M_L at $\beta = 0.80, 1.10, 1.50$ in Z(5) on a 64^2 lattice.

algorithm; in Sec. III we introduce the observables adopted in this work and study the transition from the high-temperature to the massless phase; in Sec. IV we move on to consider the transition from the massless to the low-temperature ordered phase; finally, in Sec. V we draw our conclusions. In the Appendix we check the consistency of our determination of the critical couplings with the duality transformations.

II. ALGORITHM AND NUMERICAL SETUP

In this work we concentrate our attention on the model defined by Eqs. (1) and (2), with only one nonzero coupling, $\beta_1 \equiv \beta$.[1] This model is also known as the N-state ferromagnetic clock model and is a discrete version of the continuous XY (plane rotator) model. It consists of 2D planar spins restricted to N evenly spaced directions, with spin interaction energy proportional to their scalar product.

The Hamiltonian of the model is

$$H = -\beta \sum_{\langle ij \rangle} \cos\left[\frac{2\pi}{N}(s_i - s_j)\right], \quad s_i = 0, 1, \ldots, N-1,$$

(5)

---

[1] All forthcoming tables and plots refer to the case $N = 5$, but we nevertheless present all definitions and formulas for a generic N.

with summation taken over nearest-neighbor sites. For $N = 2$ this is the Ising model, whereas in the $N \to \infty$ limit we get the XY model.

Here we develop an algorithm, valid for odd N, by which an accurate numerical study of the model can be performed for $N = 5$ (i.e., the smallest N value for which the phase structure described in Sec. I holds).

Here are the steps of our cluster algorithm for the update of a spin configuration s_i:

(i) choose randomly n in the set $(0, 1, 2, \ldots, N-1)$;

(ii) build a cluster configuration according to the following probability of bond activation between neighboring sites ij

$$p_{ij} = \begin{cases} 1 - \exp(-2\beta\,\alpha_i\alpha_j) & \text{if } \alpha_i\alpha_j > 0, \\ 0 & \text{otherwise,} \end{cases}$$

$$\text{with } \alpha_k \equiv \sin\left[\frac{2\pi}{N}(s_k - n)\right];$$

(iii) flip each cluster with probability $1/2$ by replacing all its spins according to the transformation

$$s_i \to \mathrm{mod}(-s_i + 2n + N, N),$$

which amounts to replacing each spin s_i in a cluster by the spin s_j for which $\alpha_j = -\alpha_i$. Equivalently, if the spins are mapped into the N roots of unity in the complex plane, the
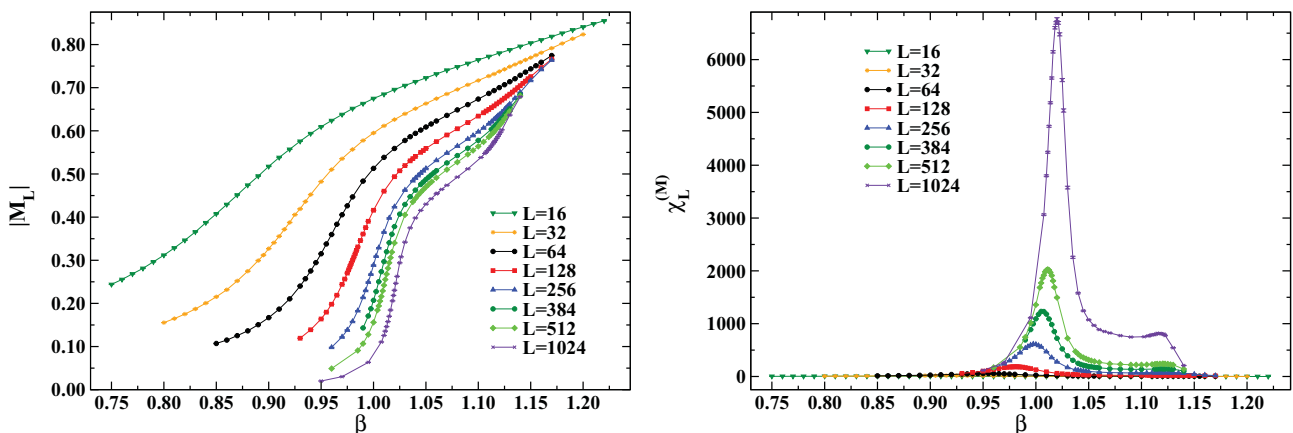

FIG. 2. (Color online) Behavior of $|M_L|$ (left) and of its susceptibility $\chi_L^{(M)}$ (right) versus β in Z(5) on lattices with L ranging from 16 to 1024.
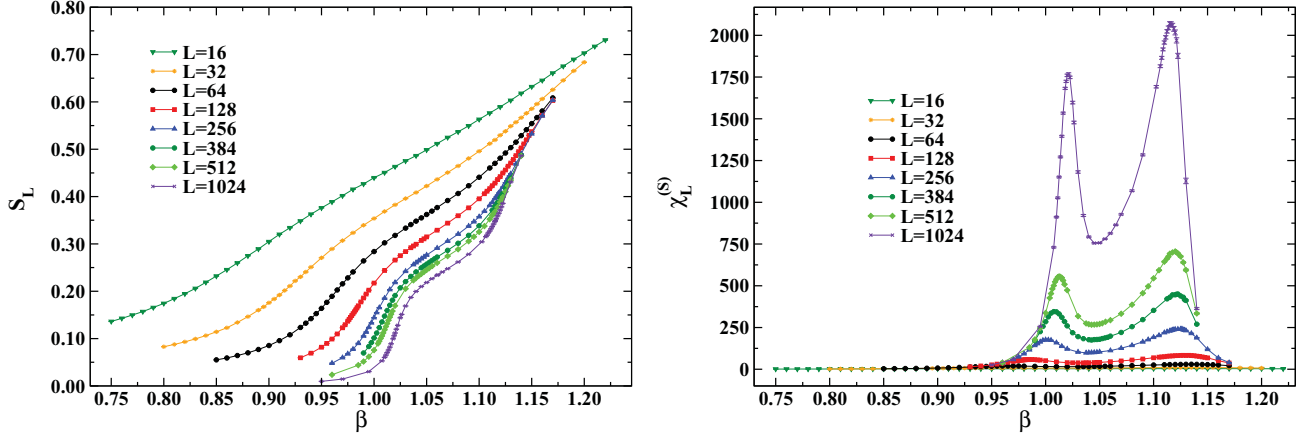
FIG. 3. (Color online) Behavior of S_L (left) and of its susceptibility $\chi_L^{(S)}$ (right) versus β in Z(5) on lattices with L ranging from 16 to 1024.

above replacement means flipping the component of each spin transverse to the direction identified by n.

It is easy to prove that this cluster algorithm fulfills the detailed balance.

We have tested the efficiency of the cluster algorithm against the standard heat-bath algorithm. On a lattice with $L = 64$ we simulated the model with $N = 5$ and determined the autocorrelation time τ of three observables: the energy, defined in Eq. (5), the magnetization M_L, and the population S_L, to be defined below. We considered three β values (0.80, 1.10, and 1.50) lying in the high-temperature, massless, and low-temperature phase of the model, respectively. Results are summarized in Table I, whose last two columns also give the number of sweeps needed to reach thermal equilibrium and the computer time to collect 50 000 statistics.

At $\beta = 0.80$ and $\beta = 1.10$ the autocorrelation time in the cluster algorithm is lower than in the heat-bath for the energy and much lower for magnetization and population. At $\beta = 1.50$, deep in the low-temperature ordered phase, τ is systematically higher in the cluster than in the heat-bath. This is a consequence of the lowering of the bond activation probability for increasing β. This drawback, however, is compensated by the higher simulation speed, with respect to the heat-bath algorithm. Moreover since the two transitions in the 2D Z(5) model are rather close (see Sections III and IV), there is no doubt that the cluster algorithm is strongly preferable.

The improvement brought along by the cluster algorithm becomes more visible when the dynamical critical exponent z is considered, defined as $\tau \sim \xi^z$, where ξ is the correlation length. We have evaluated z in the 2D Z(5) model on lattices with $L = 16, 32, 64, 128, 256, 384, 512$ at both transition points, using the autocorrelation time of the magnetization M_L. Since the correlation length diverges at both points, the expected scaling law becomes $\tau \sim L^z$. In all cases we found that τ keeps almost constant at ≈ 7, implying $z \simeq 0$ (i.e., no critical slowing down).

The three phases exhibited by the 2D Z(5) spin model can be characterized by means of two observables: the complex magnetization M_L and the population S_L.

The complex magnetization is given by

$$M_L = \frac{1}{L^2} \sum_i \exp\left(i \frac{2\pi}{N} s_i\right) \equiv |M_L| e^{i\psi}. \tag{6}$$

In Fig. 1 we show the scatter plot of M_L on a lattice with $L = 64$ in Z(5) at three values of β, each representative of a different phase: $\beta = 0.80$ (high-temperature, disordered phase), $\beta = 1.10$ (BKT massless phase), and $\beta = 1.50$ (low-temperature, ordered phase). As shown, we pass from a uniform distribution (low β) to a ring distribution (intermediate β) and finally to five isolated spots (high β).

The naive average of the complex magnetization constantly gives zero, therefore M_L is not an order parameter. Instead, an observable to detect the transition from one phase to the other is the absolute value $|M_L|$ of the complex magnetization. In Fig. 2 we show the behavior of $|M_L|$ and of its susceptibility,

$$\chi_L^{(M)} = L^2(\langle |M_L|^2 \rangle - \langle |M_L| \rangle^2), \tag{7}$$

in Z(5) on lattices with L ranging from 16 to 1024 over a wide interval of β values. On each lattice the susceptibility $\chi_L^{(M)}$ clearly exhibits two peaks, the first of them, more pronounced than the second, identifies the pseudocritical coupling $\beta_{pc}^{(1)}(L)$ at which the transition from the disordered to the massless phase occurs, whereas the second corresponds to the pseudocritical coupling $\beta_{pc}^{(2)}(L)$ of the transition from the massless to the ordered phase. It is evident from Fig. 2 that $|M_L|$ is particularly sensitive to the first transition, thus making this observable the best candidate for studying its properties.

As the order parameter to better detect the second transition (i.e., that from the massless to the ordered phase) we chose instead the population S_L, defined as

$$S_L = \frac{N}{N-1} \left[\frac{\max_{i=0,N-1}(n_i)}{L^2} - \frac{1}{N} \right], \tag{8}$$

where n_i represents the number of spins of a given configuration which are in the state s_i. In a phase in which there is not a preferred spin direction in the system (disorder), we have $n_i \sim L^2/N$ for each index i, therefore $S_L \sim 0$. Otherwise, in a phase in which there is a preferred spin direction (order), we

TABLE II. Values of $\beta_{pc}^{(1)}$ in Z(5) on L^2 lattices. The last two columns give the susceptibility $\chi_L^{(M)}$ and the magnetization $|M_L|$ at the infinite-volume coupling constant $\beta_c^{(1)} = 1.0510$.

L	$\beta_{pc}^{(1)}$	$\chi_L^{(M)}(\beta_c^{(1)})$	$|M_L|(\beta_c^{(1)})$
16	0.8523(20)	—	—
32	0.91429(90)	—	—
64	0.95373(40)	—	—
128	0.98054(30)	—	—
256	0.99838(20)	—	—
384	1.00621(10)	187.9(1.2)	0.48929(13)
512	1.01112(20)	311.5(2.0)	0.47181(13)
640	—	458.6(3.4)	0.45918(11)
768	—	631.3(4.2)	0.44863(11)
896	—	824.4(5.2)	0.44004(11)
1024	1.01991(10)	1040.0(6.9)	0.43277(11)

have $n_i \sim L^2$ for a given index i, therefore $S_L \sim 1$. In Fig. 3 we show the behavior of S_L and of its susceptibility

$$\chi_L^{(S)} = L^2 \left(\langle S_L^2 \rangle - \langle S_L \rangle^2 \right), \qquad (9)$$

in Z(5) on lattices with L ranging from 16 to 1024 over a wide interval of β values. Again the peaks signaling the two transitions are clearly visible and their positions agree with Fig. 2, but now the second one is more pronounced. Other observables which have been used in this work are the real part of the rotated magnetization, $M_R = |M_L| \cos(N\psi)$, and the order parameter introduced in Ref. [20], $m_\psi = \cos(N\psi)$, where ψ is the phase of the complex magnetization defined in Eq. (6).

In the next two sections we will study separately the two transitions of 2D Z(5) and determine some of the related critical indices. For all observables considered in this work we typically collected 100 000 measurements, on configurations separated by ten updating sweeps. For each new run the first 10 000 configurations were discarded to ensure thermalization. Data analysis was performed by the jackknife method over bins at different blocking levels.
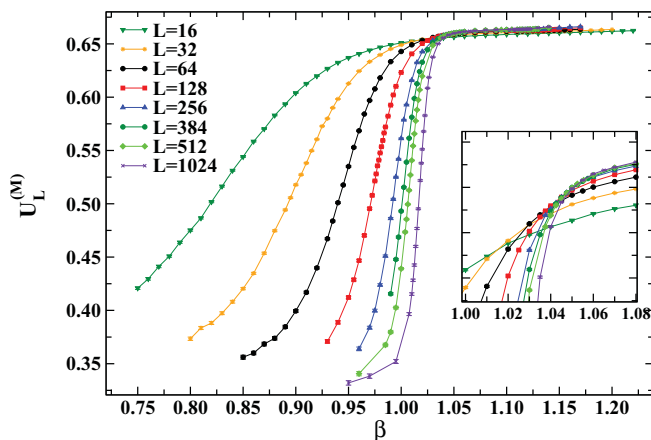

FIG. 4. (Color online) Reduced fourth-order Binder cumulant $U_L^{(M)}$ versus β on lattices with L ranging from 16 to 1024.
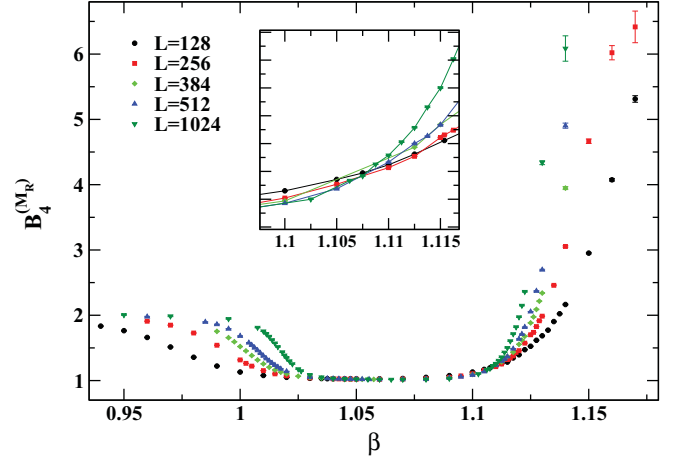

FIG. 5. (Color online) Binder cumulant $B_4^{(M_R)}$ versus β on lattices with L ranging from 128 to 1024.

III. THE TRANSITION FROM THE HIGH-TEMPERATURE TO THE MASSLESS PHASE

The first inflection point in the plot of the magnetization $|M_L|$ and the first peak in the plot of the susceptibility $\chi_L^{(M)}$ (see Fig. 2) indicate the transition from the disordered to the massless phase. The couplings where this transition occurs [denoted as the pseudocritical couplings $\beta_{pc}^{(1)}(L)$] have been determined by a Lorentzian interpolation around the peak of the susceptibility $\chi_L^{(M)}$. Their values are summarized in the second column of Table II. We observe that when the lattice size L grows, $\beta_{pc}^{(1)}(L)$ increases toward the infinite-volume critical coupling $\beta_c^{(1)}$ and that the susceptibility $\chi_L^{(M)}$ goes to zero less rapidly for $\beta > \beta_{pc}^{(1)}$, as expected in the BKT scenario.

In order to apply the finite-size scaling (FSS) program, the location of the infinite-volume critical coupling $\beta_c^{(1)}$ is needed. In Refs. [23,24] this was done by extrapolating the pseudocritical couplings to the infinite-volume limit, according to a suitable scaling law. First-order transition is ruled out by the data in Table II. Second-order transition, though not incompatible with the data in Table II, is to be
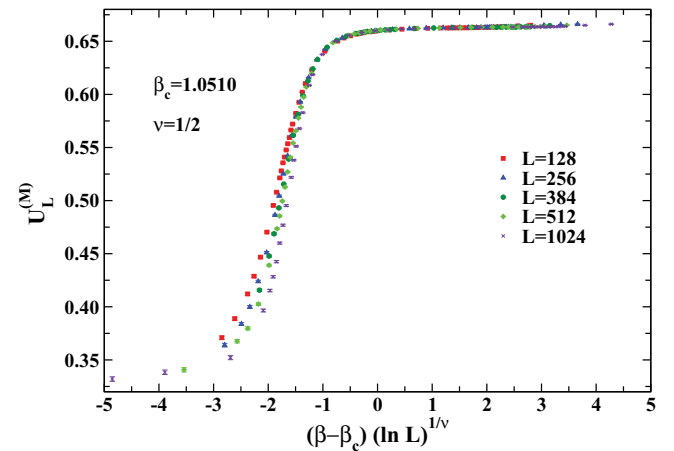

FIG. 6. (Color online) Reduced fourth-order Binder cumulant $U_L^{(M)}$ versus $(\beta - \beta_c)(\ln L)^{1/\nu}$, for $\beta_c = 1.0510$ and $\nu = 1/2$ on lattices with L ranging from 128 to 1024.

TABLE III. Results of the fit to the data of $|M_L|(\beta_c^{(1)})$ with the scaling law [Eq. (13)] on L^2 lattices with $L \geqslant L_{\min}$.

$L_{\min}$	A	β/ν	χ^2/N_{DOF}
384	1.0299(21)	0.12508(32)	1.3
512	1.0294(32)	0.12501(47)	1.7
640	1.0371(49)	0.12610(71)	0.40
768	1.0305(89)	0.1252(13)	0.021

excluded due to the vanishing of the long-distance correlations combined with the clusterization property (we will come back to this point in Sec. V). Therefore, we assume that the transition is of the BKT type and adopt the scaling law dictated by the essential scaling of the BKT transition (i.e., $\xi \sim e^{bt^{-\nu}}$) which reads

$$\beta_{\mathrm{pc}}^{(1)} = \beta_c^{(1)} + \frac{A}{(\ln L + B)^{1/\nu}}. \tag{10}$$

The index ν characterizes the universality class of the system. For example, $\nu = 1/2$ holds for the 2D XY universality class.

Unfortunately, four-parameter fits of the data for $\beta_{\mathrm{pc}}^{(1)}(L)$ give very unstable results for the parameters. This led us to move to three-parameter fits of the data, with ν fixed at $1/2$. We found, as best fit with the MINUIT optimization code,

$$\beta_c^{(1)} = 1.0602(20), \quad A_1 = -2.09(20), \quad B_1 = 0.27(18),$$

$\chi^2/N_{\mathrm{DOF}} = 0.48$ (where N_{DOF} indicates degrees of freedom),

$$L_{\min} = 64.$$

We observe that $\beta_c^{(1)}$ is rather far from the value of $\beta_{\mathrm{pc}}^{(1)}$ on the largest available lattice, thus casting some doubts on the reliability of the extrapolation to the thermodynamic limit. For this reason, we turned to an independent method for the determination of $\beta_c^{(1)}$, based on the use of Binder cumulants.

In particular, we considered the reduced fourth-order Binder cumulant $U_L^{(M)}$ defined as

$$U_L^{(M)} = 1 - \frac{\langle |M_L|^4 \rangle}{3 \langle |M_L|^2 \rangle^2}, \tag{11}$$

and the cumulant $B_4^{(M_R)}$ defined as

$$B_4^{(M_R)} = \frac{\langle |M_R - \langle M_R \rangle|^4 \rangle}{\langle |M_R - \langle M_R \rangle|^2 \rangle^2}. \tag{12}$$

Plots of the various Binder cumulants versus β show that data obtained on different lattice volumes align on curves that cross in two points, corresponding to the two transitions (see Figs. 4 and 5). We used also the reduced fourth-order Binder cumulant of the action which showed no crossing points nor

TABLE IV. Results of the fit to the data of $\chi_L^{(M)}(\beta_c^{(1)})$ with the scaling law [Eq. (14)] on L^2 lattices with $L \geqslant L_{\min}$.

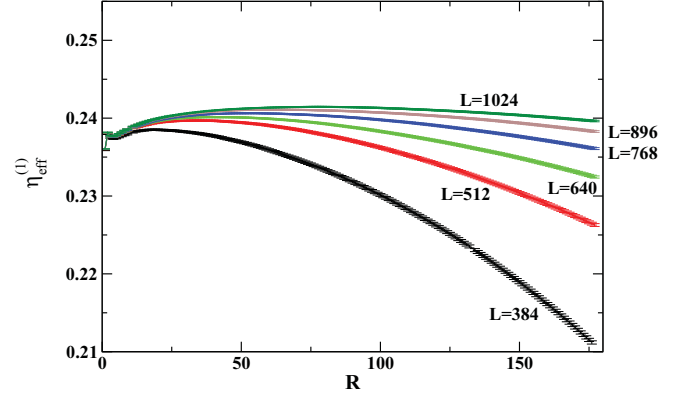| $L_{\min}$	A	γ/ν	χ^2/N_{DOF}
384	0.00586(30)	1.7438(80)	0.060
512	0.00602(48)	1.740(12)	0.018
640	0.00598(81)	1.741(20)	0.025
768	0.0062(14)	1.735(34)	0.0063

FIG. 7. (Color online) $\eta_{\mathrm{eff}}^{(1)}$ versus R at $\beta_c^{(1)} = 1.0510$ on lattices with $L = 384, 512, 640, 768, 896, 1024$.

volume-dependent dips, thus confirming the absence of first-order phase transitions.

We determined the crossing point by plotting the Binder cumulants versus $(\beta - \beta_c)(\ln L)^{1/\nu}$, with ν fixed at $1/2$, and by looking for the optimal overlap of data from different lattices using the χ^2 method (see Fig. 6 for an example of this kind of plot). As a result of this analysis we arrived at the following estimate: $\beta_c^{(1)} = 1.0510(10)$. We observe that $\beta_c^{(1)}$ is not compatible with the infinite-volume extrapolation of the corresponding pseudocritical couplings, thus confirming our previous worries about the safety of the infinite-volume extrapolation of $\beta_{\mathrm{pc}}^{(1)}$. It should be noted, however, that a fit to $\beta_{\mathrm{pc}}^{(1)}(L)$ with the law (10) and with $\beta_c^{(1)}$ fixed at 1.0510 and ν fixed at $1/2$ gives a good χ^2/N_{DOF} if only the three largest volumes are considered in the fit.

We have also tested the strong-coupling prediction of Ref. [5] suggesting $\nu = 0.22$. In particular, we have plotted the Binder cumulant $U_L^{(M)}$ versus $(\beta - \beta_c)(\ln L)^{1/\nu}$, with ν fixed now at the candidate value 0.22. We have seen that when β_c varies on a wide interval the overlap among curves from different lattices is always rather poor.

We are now in the position to extract other critical indices and thus check the hyperscaling relation. According to the

TABLE V. Values of $\beta_{\mathrm{pc}}^{(2)}$ in Z(5) on L^2 lattices. The last two columns give the susceptibility $\chi_L^{(M_R)}$ and the rotated magnetization M_R at the infinite-volume coupling constant $\beta_c^{(2)} = 1.1048$.

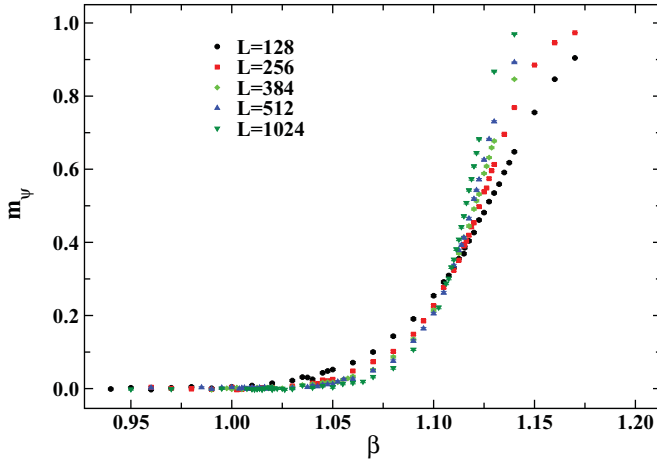| L	$\beta_{\mathrm{pc}}^{(2)}$	$\chi_L^{(M_R)}(\beta_c^{(2)})$	$M_R(\beta_c^{(2)})$
16	1.1323(19)	–	–
32	1.1363(11)	–	–
64	1.13212(60)	–	–
128	1.12875(66)	–	–
256	1.12290(16)	–	–
384	1.12103(50)	47116(77)	0.1618(18)
512	1.11912(28)	80057(139)	0.1575(19)
640	–	120777(229)	0.1557(20)
768	–	169358(298)	0.1517(19)
896	–	224879(339)	0.1502(16)
1024	1.11596(38)	288151(532)	0.1473(18)

FIG. 8. (Color online) Behavior of m_ψ versus β on lattices with L ranging from 128 to 1024.

standard FSS theory, in an $L \times L$ lattice at criticality the equilibrium magnetization $|M_L|$ should obey the relation $|M_L| \sim L^{-\beta/\nu}$ for sufficiently large L.[2] We performed a fit to the data of $|M_L|(\beta_c^{(1)})$ (reported in the last column of Table II) on all lattices with size L not smaller than a given $L_{\min}$ according to the scaling law

$$|M_L| = AL^{-\beta/\nu} \tag{13}$$

and summarized our results in Table III.

The FSS behavior of the $\chi_L^{(M)}$ susceptibility defined in Eq. (7) is given by $\chi_L^{(M)} \sim L^{\gamma/\nu}$, where $\gamma/\nu = 2 - \eta$ and η is the magnetic critical index. We performed a fit to the data of $\chi_L^{(M)}(\beta_c^{(1)})$ (reported in the third column of Table II) on all lattices with size L not smaller than a given $L_{\min}$ according to the scaling law

$$\chi_L^{(M)} = AL^{\gamma/\nu} \tag{14}$$

and summarized our results in Table IV. As we can see, for all values of $L_{\min}$ considered, the value of the magnetic index[3] $\eta^{(1)} \equiv 2 - \gamma/\nu$ is compatible with 1/4. Note also that the hyperscaling relation $\gamma/\nu + 2\beta/\nu = d$, where d is

———————

[2]The symbol β here denotes a critical index and not, obviously, the coupling of the theory. In spite of this inconvenient notation, we are confident that no confusion will arise, since it will always be clear from the context which β is to be referred to.

[3]The notation $^{(1)}$ in η means "at the infinite-volume critical coupling of the first transition."

TABLE VI. Results of the fit to the data of $\chi_L^{(M_R)}(\beta_c^{(2)})$ with the scaling law (14) on L^2 lattices with $L \geqslant L_{\min}$.

$L_{\min}$	A	γ/ν	χ^2/N_{DOF}
384	0.799(11)	1.8459(21)	0.23
512	0.791(17)	1.8473(32)	0.19
640	0.784(28)	1.8487(53)	0.22
768	0.793(50)	1.8470(92)	0.39

TABLE VII. Results of the fit to the data of $M_R(\beta_c^{(2)})$ with the scaling law (13) on L^2 lattices with $L \geqslant L_{\min}$.

$L_{\min}$	A	β/ν	χ^2/N_{DOF}
384	0.281(26)	0.093(14)	0.15
512	0.288(41)	0.096(22)	0.18
640	0.322(77)	0.112(36)	0.12
768	0.30(12)	0.102(60)	0.19

the dimension of the system, is always satisfied within the statistical error.

An independent determination of the magnetic index η can be achieved by the approach developed in Ref. [23]. An effective η index is defined through the spin-spin correlation function $\Gamma(R)$, according to

$$\eta_{\mathrm{eff}}^{(1)}(R) \equiv \frac{\ln[\Gamma(R)/\Gamma(R_0)]}{\ln[R_0/R]}, \tag{15}$$

with R_0 chosen equal to 10, as in Ref. [23]. This quantity is constructed in such a way that it exhibits a plateau in R if the correlator obeys the law

$$\Gamma(R) \asymp \frac{1}{R^{\eta(T)}}, \tag{16}$$

valid in the BKT phase, $\beta \geqslant \beta_c^{(1)}$. In Fig. 7 we show the behavior of $\eta_{\mathrm{eff}}^{(1)}(R)$ at the infinite-volume critical coupling $\beta_c^{(1)} = 1.0510$ on lattices with $L = 384, 512, 640, 768, 896, 1024$. It turns out that a plateau develops at small distances when L increases and that the extension of this plateau gets larger with L, consistent with the fact that finite-volume effects are becoming less important. The plateau value of $\eta_{\mathrm{eff}}^{(1)}$ can be estimated at about 0.24. We checked that this result is stable under variation of the parameter R_0. The discrepancy with the expected value of 1/4 can be explained by the imperfect localization of the critical point and (or) by the effect of logarithmic corrections [25,26] that we were not able to include in our analysis.

IV. THE TRANSITION FROM THE MASSLESS TO THE LOW-TEMPERATURE ORDERED PHASE

The second inflection point in the plot of the population S_L and the second peak in the plot of the susceptibility $\chi_L^{(S)}$ (see Fig. 3) indicate the transition from the massless to the ordered phase. The couplings where this transition occurs [denoted as the pseudocritical couplings $\beta_{\mathrm{pc}}^{(2)}(L)$] have been determined by a Lorentzian interpolation around the peak of the susceptibility $\chi_L^{(S)}$. Their values are summarized in the second column of Table V.

Available results [5,11] suggest that the correlation length diverges according to the essential scaling scenario when the critical point is approached from above. Our aim is to check the validity of this statement and then extract relevant indices characterizing the system at this transition. Again, first-order transition is ruled out by the data in Table V (and by the aforementioned analysis of the Binder cumulant of the action), while second-order transition is not. We assume that a BKT transition is at work here and, therefore, that pseudocritical couplings scale with L according to the law (10). As before,
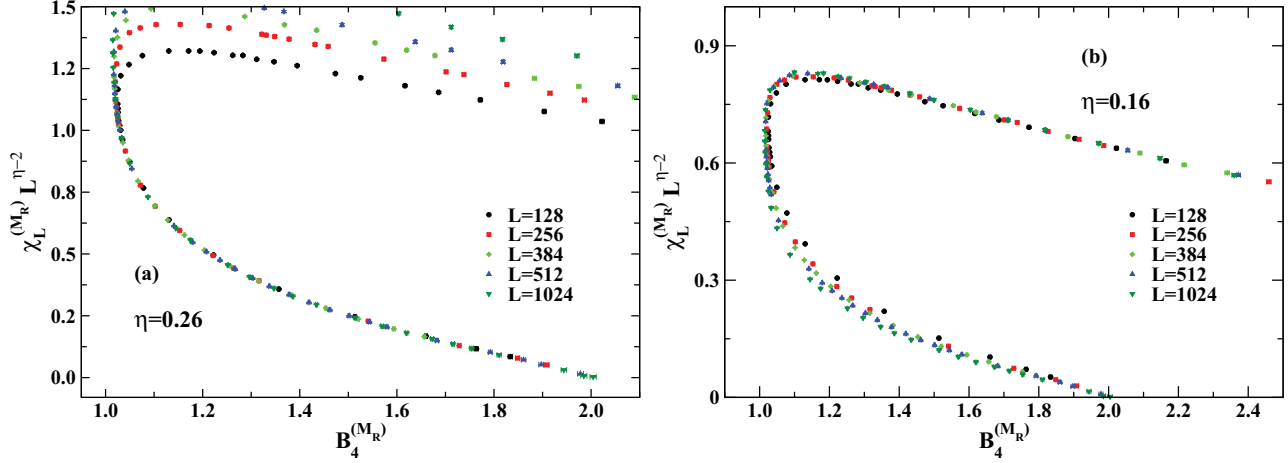
FIG. 9. (Color online) Correlation between $\chi_L^{(M_R)} L^{\eta-2}$ and the Binder cumulant $B_4^{(M_R)}$ for (a) $\eta = 0.26$ and (b) $\eta = 0.16$ on lattices with L ranging from 128 to 1024. For $\eta = 0.26$ (a) data from different lattices tend to fall on a universal curve in the lower branch, corresponding to β values in the region of the first transition. For $\eta = 0.16$ (b) data from different lattices tend to fall on a universal curve in the upper branch, corresponding to β values in the region of the second transition.

four-parameter fits of the data for $\beta_{\mathrm{pc}}^{(2)}(L)$ are unstable and we moved to three-parameter fits of the data, with ν fixed at $1/2$, and found that the parameter B_2 turns out to be compatible with zero so that, in fact, a two-parameter fit works well:

$$\beta_c^{(2)} = 1.1042(12), \quad A_2 = 0.578(41), \quad B_2 = 0,$$

$$\chi^2/N_{\mathrm{DOF}} = 0.61, \quad L_{\min} = 128.$$

Now $\beta_c^{(2)}$ is not far from the value of $\beta_{\mathrm{pc}}^{(2)}$ on the largest available lattice, thus supporting the reliability of the extrapolation to the thermodynamic limit.

In order to localize the critical coupling $\beta_c^{(2)}$, we looked for the crossing point at higher β of the Binder cumulant $B_4^{(M_R)}$ defined in Eq. (12) and repeated the analysis based on the optimal overlap of data points when they are plotted against $(\beta - \beta_c)(\ln L)^{1/\nu}$, with ν fixed at $1/2$. The same procedure was also carried out using the observable m_ψ, which is itself an RG-invariant quantity and therefore shares the same properties as a Binder cumulant (see Fig. 8 for the behavior of m_ψ versus β on various lattices, which shows

two crossing points, the one at higher β corresponding to the transition from the massless to the ordered phase). This analysis led to the result $\beta_c^{(2)} = 1.1048(10)$, which agrees with the infinite-volume extrapolation of the corresponding pseudocritical couplings.

We can now determine the ratios of critical indices β/ν and γ/ν as we did in Sec. III. It should be noted, however, that the population S_L and its susceptibility are not suitable observables for this purpose, since they are defined in a nonlocal manner and, thus, not directly related to the two-point correlator. Instead we use the rotated magnetization M_R and its susceptibility $\chi_L^{(M_R)}$ and compare their values at the infinite-volume critical coupling $\beta_c^{(2)}$ (see the last two columns of Table V) with the scaling laws (13) and (14), respectively. Results for β/ν and γ/ν are summarized in Tables VI and VII. All the values for $\eta^{(2)} = 2 - \gamma/\nu$ given in Table VI are in agreement with the prediction $4/N^2$, which gives 0.16 for $N = 5$. The hyperscaling relation $\gamma/\nu + 2\beta/\nu = d$ is always satisfied within the statistical error.
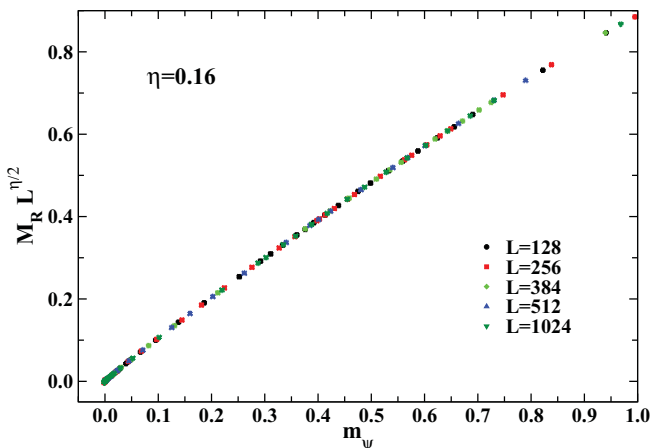

FIG. 10. (Color online) Correlation between $M_R L^{\eta/2}$ and m_ψ for $\eta = 0.16$ on lattices with L ranging from 128 to 1024.
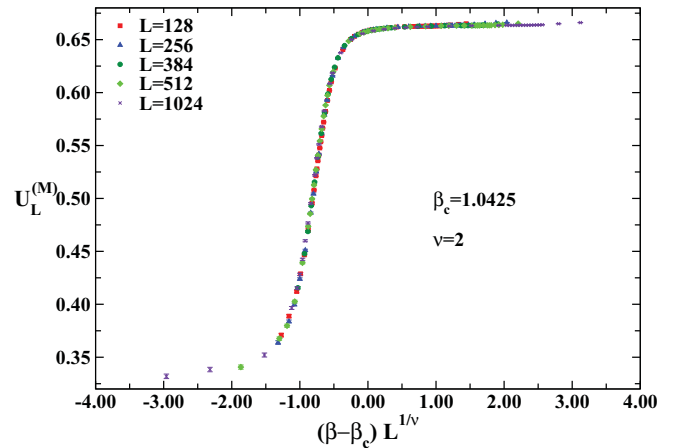

FIG. 11. (Color online) Reduced fourth-order Binder cumulant $U_L^{(M)}$ versus $(\beta - \beta_c)L^{1/\nu}$, for $\beta_c = 1.0425$ and $\nu = 2$ on lattices with L ranging from 128 to 1024.
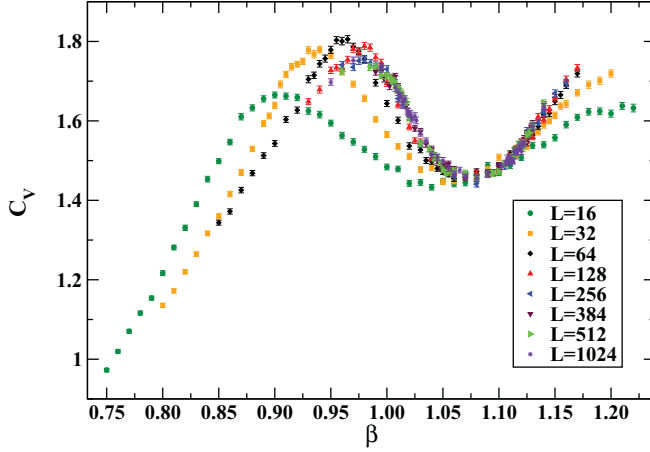
FIG. 12. (Color online) Specific heat C_V measured on lattices with L ranging from 16 to 1024.

The determination of the magnetic critical index based on the effective η index defined in (15) is plagued, in this region of values of β, by a sizable dependence on the choice of the arbitrary parameter R_0. The shape of the curves for $\eta_{\text{eff}}(R)$ and the way they depend on R_0 suggest that logarithmic corrections to the scaling could be at work here. However, our data are not accurate enough to include them reliably in our fits.

We conclude this section by presenting several examples of *a posteriori* checks of consistency of our determinations for $\eta^{(1)}$ and $\eta^{(2)}$. The basic idea is to build plots in which we correlate two RG-invariant quantities and to check that sequences of data points corresponding to different values of β fall on a universal curve, irrespective of the lattice size L [27,28].

The first example is the plot of the rescaled susceptibility $\chi_L^{(M_R)} L^{\eta-2}$ against the Binder cumulant $B_4^{(M_R)}$. One can see from Fig. 9(a) that, for $\eta = 0.26 \simeq \eta^{(1)}$, data points from different lattices fall on the same curve in the lower branch corresponding to β values in the region of the first transition. For $\eta = 0.16 \simeq \eta^{(2)}$, on the contrary, data points from different lattices fall on the same curve in the upper branch, corresponding to β values in the region of the second transition [see Fig. 9(b)].

Another example is provided by the plot of the rescaled magnetization $M_R L^{\eta/2}$ against m_ψ. For $\eta = 0.16 \simeq \eta^{(2)}$, again, data points from different lattices fall on the same curve (see Fig. 10).

V. DISCUSSION AND CONCLUSIONS

In this paper we have presented a wealth of numerical data aimed at shedding light on the phase structure of the 2D Z(5) vector model. By means of a Monte Carlo cluster updating algorithm, designed to work for Z(N) models with odd N, we have outlined a scenario compatible with the existence of three phases: disordered (small β), massless or BKT (intermediate β), ordered (large β). We have determined (i) the critical points $\beta_c^{(1)}$ and $\beta_c^{(2)}$ in the infinite-volume limit by means of the FSS of suitable Binder cumulants, and (ii) the critical indices β/ν and

γ/ν at the two critical points by means of the FSS of suitable definitions of the magnetization and of its susceptibility.

The determination of $\beta_c^{(2)}$ has been cross-checked with the infinite-volume extrapolation of the (volume-dependent) pseudocritical couplings of the second transition, assuming essential scaling. We have found the following values of the critical couplings: $\beta_c^{(1)} = 1.0510(10)$ and $\beta_c^{(2)} = 1.1048(10)$. As mentioned in Sec. I, values of the critical points are related by the duality transformations. In the Appendix we check, via the duality, the accuracy of our predictions and show that our determination of the critical couplings is in rather good agreement with it.

The determination of the index $\eta^{(1)} = 2 - \gamma/\nu$ at the first transition has been cross-checked with the effective η index method. The values of the index γ/ν at both critical points agree well with theoretical predictions obtained for the Villain formulation [5] thus supporting the conjecture that both standard and Villain formulations are in the same universality class. The behavior of the complex magnetization as well as the two-point correlation function strongly indicate that the intermediate phase is a massless phase whose symmetry is U(1). Moreover, using spin-wave–vortex approximation and conventional perturbation theory one can calculate the two-point correlation function analytically and extract the perturbative beta function in the intermediate phase. It turns out that the beta function vanishes in this phase, a property which further supports the presence of the BKT transition and massless phase.

For completeness, we have tested a scenario in which both transitions are second order. In this case, the infinite-volume extrapolation of the pseudocritical couplings should obey

$$\beta_{\text{pc}}^{(1,2)} = \beta_c^{(1,2)} + \frac{A}{L^{1/\nu}},$$

whereas the overlap method of the Binder cumulants should work when data are plotted against $(\beta - \beta_c)L^{1/\nu}$. Under these conditions, we found

$$\beta_c^{(1)} = 1.0425(25), \quad 1/\nu^{(1)} = 0.50(5),$$
$$\beta_c^{(2)} = 1.1075(25), \quad 1/\nu^{(2)} = 0.45(5).$$

In Fig. 11 we show the overlap of the curves for the Binder cumulant $U_L^{(M)}$ obtained on various lattices when plotted versus $(\beta - \beta_c)L^{1/\nu}$, with $1/\nu$ fixed at 0.5 and $\beta_c = 1.0425$. The quality of the overlap seems to be better overall than in the BKT scenario of Fig. 6, but a closer inspection shows that it is worse in the region near the critical point.

Second-order transition at $\beta_c^{(1)}$, however, should be excluded by the numerical evidence that the intermediate phase is massless. In particular, two-point correlators tend to vanish at large distances for large volumes, whereas one should expect spontaneous symmetry breaking and nonvanishing values of long-distance correlations in the case of second-order phase transition. The exclusion of the second-order transition at $\beta_c^{(2)}$ seems to be a more subtle problem, at least on the numerical side. One should probably simulate the system on larger lattices to reliably distinguish the BKT scenario from the second-order one, if we deal with the quantities studied so far. However, one could consider more traditional observables to determine the order of the phase transition. The

BKT phase transition is of infinite order. In particular, it is expected that the singular part of the free energy of the *XY* model behaves like $F_s \sim \xi^{-2}$. Hence, all derivatives of the free energy are analytic functions of the temperature. In turn, the second derivative of the free energy shows a finite jump if the system undergoes a second-order phase transition. We have decided, therefore, to compute the specific heat C_V of the Z(5) model. Figure 12 shows the result of simulations for various lattice sizes. As suggested by this plot, the specific heat shows neither a divergence nor a finite jump. We interpret this behavior as further evidence in favor of the infinite-order phase transition. On the theoretical side, the second-order transition seems incompatible with the analysis of the dual transformations [15,16].

As discussed in Sec. I, in a recent work [19] it has been claimed that the phase transition at $\beta_c^{(1)}$ is not a standard BKT phase transition. The main tool in the analysis of Ref. [19] was the helicity modulus Υ, which was not considered in this work. The key observation in Ref. [19] was that the helicity modulus does not jump to zero across the phase transition. This property prompted the authors of Ref. [19] to conclude that the phase transition at $\beta_c^{(1)}$ is a weaker cousin of the standard BKT transition. Our data indicate that such behavior of the helicity modulus seems to have no influence on other characteristic features of the phase transition. Most important is the fact that both standard and Villain formulation are still in the same universality class since they show equal critical indices. Moreover, one could consider the critical index which governs the behavior of the helicity modulus [29]

$$\Upsilon \sim \left(\frac{T - T_c}{T_c} \right)^\upsilon, \quad \upsilon = 2\beta - \eta \nu.$$

Our data for the indices β and $\eta^{(1)}$ are compatible with a vanishing value of υ. Thus, $\Upsilon = $ const right at the critical point. Obviously, $\upsilon = 0$ also for the Villain model. The nonvanishing value of Υ at $\beta < \beta_c^{(1)}$ seems to characterize the high-temperature phase rather than the massless BKT phase. Indeed, a physical interpretation given in Ref. [19] refers to the lack of free vortices in the high-temperature phase of the Z(5) models. It would then be interesting and important to study the dynamics of the vortex-antivortex pairs in both formulations. These dynamics can indeed be different. This task, however, is beyond the scope of this paper.

APPENDIX

Consider the general Z(5) vector Potts model with Boltzmann weight given by

$$Q(s) = 1 + 2x(\beta) \cos \frac{2\pi}{5}s + 2y(\beta) \cos \frac{4\pi}{5}s.$$

Duality transformations read [14]

$$x_d(\beta) = [1 + 2x(\beta)\cos(2\pi/5) + 2y(\beta)\cos(4\pi/5)]/$$
$$\times [1 + 2x(\beta) + 2y(\beta)],$$
$$y_d(\beta) = [1 + 2x(\beta)\cos(4\pi/5) + 2y(\beta)\cos(2\pi/5)]/$$
$$\times [1 + 2x(\beta) + 2y(\beta)].$$

The initial couplings $x(\beta)$ and $y(\beta)$ can be calculated from the Fourier transform of the original Boltzmann weight and in our case they are given by

$$x(\beta) = \left[-1 - \sqrt{5} + (-1 + \sqrt{5})e^{\frac{\sqrt{5}\beta}{2}} + 2e^{\frac{1}{4}(5+\sqrt{5})\beta} \right]/$$
$$\times \left[4 + 4e^{\frac{\sqrt{5}\beta}{2}} + 2e^{\frac{1}{4}(5+\sqrt{5})\beta} \right], \qquad \text{(A1)}$$
$$y(\beta) = \left[-1 + \sqrt{5} - (1 + \sqrt{5})e^{\frac{\sqrt{5}\beta}{2}} + 2e^{\frac{1}{4}(5+\sqrt{5})\beta} \right]/$$
$$\times \left[4 + 4e^{\frac{\sqrt{5}\beta}{2}} + 2e^{\frac{1}{4}(5+\sqrt{5})\beta} \right]. \qquad \text{(A2)}$$

It follows that

$$x_d(\beta) = e^{\frac{1}{4}(-5+\sqrt{5})\beta}, \qquad \text{(A3)}$$
$$y_d(\beta) = e^{-\frac{1}{4}(5+\sqrt{5})\beta}. \qquad \text{(A4)}$$

Now, consider original and dual partition functions,

$$Z[x(\beta), y(\beta)] = C(\beta) \, Z[x_d(\beta), y_d(\beta)].$$

They have the same form and differ only by a smooth function $C(\beta)$. Suppose the original partition function is critical at $\beta_c^{(1)}$ and $\beta_c^{(2)}$. These values correspond to $(x^{(1)}, y^{(1)})$ and $(x^{(2)}, y^{(2)})$. Let $(x_d^{(1)}, y_d^{(1)})$ and $(x_d^{(2)}, y_d^{(2)})$ be the values of dual couplings at critical points. The interaction in the original and dual partition functions is the same. Therefore, numerical values of the critical points in terms of (x, y) and (x_d, y_d) should be the same. However, we know from the solution of the self-dual equation (see [14]) that the self-dual point is not a critical point for the vector Potts model. This leaves only one possibility: at the critical points one must have

$$x^{(1)} = x_d^{(2)}, \quad y^{(1)} = y_d^{(2)}$$

and

$$x^{(2)} = x_d^{(1)}, \quad y^{(2)} = y_d^{(1)}.$$

Results for critical points reported in the text are $\beta_c^{(1)} = 1.051$ and $\beta_c^{(2)} = 1.1048$. So, we easily find from Eqs. (A1)–(A4)

$$x(1.051) = 0.466\,532, \quad x_d(1.1048) = 0.466\,08$$
$$y(1.051) = 0.136\,626, \quad y_d(1.1048) = 0.135\,523$$

and

$$x(1.1048) = 0.485\,097, \quad x_d(1.051) = 0.483\,733$$
$$y(1.1048) = 0.149\,612, \quad y_d(1.051) = 0.149\,378.$$

[1] V. L. Berezinskii, Sov. Phys. JETP **32**, 493 (1971).

[2] J. Kosterlitz and D. Thouless, J. Phys. C **6**, 1181 (1973).

[3] J. Kosterlitz, J. Phys. C **7**, 1046 (1974).

[4] F. Y. Wu, Rev. Mod. Phys. **54**, 235 (1982).

[5] S. Elitzur, R. B. Pearson, and J. Shigemitsu, Phys. Rev. D **19**, 3698 (1979).

[6] M. B. Einhorn, R. Savit, and E. Rabinovici, Nucl. Phys. B **170**, 16 (1980)

[7] C. J. Hamer and J. B. Kogut, Phys. Rev. B **22**, 3378 (1980).

[8] B. Nienhuis, J. Stat. Phys. **34**, 731 (1984).

[9] L. P. Kadanoff, J. Phys. A **11**, 1399 (1978).

[10] J. Fröhlich and T. Spencer, Commun. Math. Phys. **81**, 527 (1981).

[11] Y. Tomita and Y. Okabe, Phys. Rev. B **65**, 184405 (2002).

[12] B. Svetitsky and L. Yaffe, Nucl. Phys. B **210**, 423 (1982).

[13] A. Ukawa, P. Windey, and A. H. Guth, Phys. Rev. D **21**, 1013 (1980).

[14] F. Y. Wu, J. Phys. C **12**, L317 (1979).

[15] J. L. Cardy, J. Phys. A **13**, 1507 (1980).

[16] E. Domany, D. Mukamel, and A. Schwimmer, J. Phys. A **13**, L311 (1980).

[17] P. Ruján, G. O. Williams, H. L. Frisch, and G. Forgács, Phys. Rev. B **23**, 1362 (1981); H. H. Roomany and H. W. Wyld, *ibid.* **23**, 1357 (1981).

[18] C. M. Lapilli, P. Pfeifer, and C. Wexler, Phys. Rev. Lett. **96**, 140603 (2006).

[19] S. K. Baek and P. Minnhagen, Phys. Rev. E **82**, 031102 (2010).

[20] S. K. Baek, P. Minnhagen, and B. J. Kim, Phys. Rev. E **80**, 060101(R) (2009).

[21] M. Hasenbusch, J. Stat. Mech. (**2008**) P08003.

[22] O. Borisenko, G. Cortese, R. Fiore, M. Gravina, and A. Papa, *Proceedings of the 28th International Symposium on Lattice Field Theory, Villasimius, Italy, 2010*, edited by A. Vladikas *et al.*, PoS(Lattice2010), 274.

[23] O. Borisenko, M. Gravina, and A. Papa, J. Stat. Mech. (2008) P08009.

[24] O. Borisenko, R. Fiore, M. Gravina, and A. Papa, J. Stat. Mech. (2010) P04015.

[25] R. Kenna and A. C. Irving, Nucl. Phys. B **485**, 583 (1997).

[26] M. Hasenbusch, J. Phys. A **38**, 5869 (2005).

[27] M. S. S. Challa, D. P. Landau, and K. Binder, Phys. Rev. B **34**, 1841 (1986).

[28] D. Loison, J. Phys.: Condens. Matter **11**, L401 (1999).

[29] M. E. Fisher, M. N. Barber, and D. Jasnow, Phys. Rev. A **8**, 1111 (1973).